ANTIOXIDANTS & REDOX SIGNALING
Volume 10, Number 3, 2008

DOI: 10.1089/ars.2007.1821

Original Research Communication

Expression Pattern of Human Glutaredoxin 2 Isoforms: Identification and Characterization of Two Testis/Cancer Cell-Specific Isoforms

MARIA ELISABET LÖNN,[1] CHRISTOPH HUDEMANN,[1] CARSTEN BERNDT,[1,3] VALERIA CHERKASOV,[3] FRANCISCO CAPANI,[2] ARNE HOLMGREN,[1] and CHRISTOPHER HORST LILLIG[1,3]

ABSTRACT

The cellular redox state is associated with major cellular processes including differentiation, transformation, and apoptosis. Glutaredoxin 2 (Grx2) is a mitochondrial oxidoreductase suggested to play a critical role in protection against apoptotic stimuli. An alternative Grx2 transcript variant encoding a nonmitochondrial protein (Grx2b) was proposed before, but no data was available on the expression of this isoform. We have systematically investigated the expression of Grx2 transcript variants in human tissues and transformed cell lines. The transcript variant encoding mitochondrial Grx2 (Grx2a) was found to be ubiquitously expressed, emphasizing the general importance of the protein for mitochondrial redox homeostasis. In addition, we confirmed the previously suggested isoform Grx2b and identified a new third isoform (Grx2c) derived from alternative splicing of the Grx2b-encoding transcript. In normal tissue expression of both Grx2b and Grx2c was restricted to testes, but additionally we were able to demonstrate transcripts in various cancer cell lines. Both Grx2b and Grx2c are enzymatically active, but only Grx2c can complex the regulatory iron–sulfur cluster described for Grx2a. Expression of GFP fusion proteins suggested a cytosolic and nuclear localization of both Grx2b and Grx2c. Our findings provide the first evidence for functions of Grx2 outside mitochondria. *Antioxid. Redox Signal.* 10, 547–557.

INTRODUCTION

Glutaredoxins (Grxs) are thiol–disulfide oxidoreductases and part of the thioredoxin (Trx) family of proteins. Grxs are glutathione (GSH)-dependent enzymes involved in the maintenance of cellular redox homeostasis. The proteins react via a monothiol or dithiol mechanism utilizing one or two cysteines in their Cys–Pro–Tyr–Cys active site (5, 11, 30, 45). First discovered as electron donor for ribonucleotide reductase (RNR) (14, 15), Grxs are almost ubiquitously present in a growing number of isoforms in most species (51).

In mammals, two Grxs containing the dicysteine motif in their active site have been identified. Cytosolic Grx1 supports RNR with electrons and is involved in multiple redox-controlled cellular processes (*e.g.*, dehydroascorbate reduction, cellular differentiation, regulation of transcription factors, and apoptosis) (25, 44). The second mammalian Grx (Grx2) was suggested to be present in at least two alternatively transcribed mRNA

[1]The Medical Nobel Institute for Biochemistry, Department of Medical Biochemistry and Biophysics, Karolinska Institutet, Stockholm, Sweden.
[2]The Department of Cell Biology and Histology, School of Medicine, University of Buenos Aires, Buenos Aires, Argentina.
[3]The Institute for Clinical Cytobiology and Cytopathology, Philipps University, Marburg, Germany.
Maria Elisabet Lönn and Christoph Hudemann contributed equally to this work.

isoforms (10, 28). The human Grx2 gene (GLRX2) is located on chromosome 1 (1q31.2-31.3) and consists of five exons. Exons II to IV form the Grx core, with the unusual active site (Cys–Ser–Tyr–Cys) encoded by exon III. The characteristic GSH-binding motifs are encoded by exons III and IV. Exon Ia encodes a mitochondrial translocation signal; a second putative Grx2 isoform (Grx2b) containing the alternative exon Ib was suggested to be targeted to the nucleus (28).

Mitochondrial Grx2 (Grx2a) was suggested to play a central role in mitochondrial redox homeostasis by catalyzing the reversible glutathionylation/de-glutathionylation of protein thiols (2). HeLa cells, in which the expression of Grx was silenced by RNA interference, were dramatically sensitized to cell death induced by oxidative stress-inducing apoptotic agents (26). The EC_{50} for the anticancer drug doxorubicin/adriamycin decreased 60-fold and the EC_{50} for phenylarsine oxide, a compound that blocks specifically vicinal dithiols, 40-fold. Corroboratively, overexpression of Grx2 decreased the susceptibility of HeLa cells to apoptosis induced by doxorubicin and the antimetabolite 2-deoxy-D-glucose (8). Grx2 prevented loss of cardiolipin, inhibited cytochrome *c* release, and caspase activation. Overexpression of mitochondrial Grx2a provided better protection than overexpression of a cytosolic mutant lacking the mitochondrial translocation signal (8).

Complex I of the inner mitochondrial membrane is the major source of reactive oxygen species (ROS) for most cells. ROS production results in a decreased ratio of reduced GSH to glutathione disulfide (GSSG) which in turn affects the activity of many key proteins by formation of mixed disulfides of GSH with critical Cys residues (9, 16, 25, 44). ROS production by complex I correlates with the formation of mixed disulfides of two Cys residues in its NADH binding pocket with GSH (49). Grx2 efficiently catalyzes the reduction of GSH-mixed disulfides (19). In fact, Grx2 catalyzes the reversible glutathionylation of complex I under oxidizing conditions. Thus, Grx2 may link the mitochondrial response to redox signals and oxidative stress (2). Unlike other Grxs, Grx2 can receive electrons not only from GSH but also from the seleno-enzyme thioredoxin reductase (TrxR) (19). This alternative electron pathway may come into play when the GSH/GSSG ratio or the intracellular pH drops, conditions when Grxs that rely solely on GSH as electron donor are inactive (15). Human Grx2 was described as the first iron–sulfur protein from the thioredoxin family of proteins. The protein can exist in both the apo- and the dimeric [2Fe-2S] holo-form. Specific co-immunoprecipitation of iron with Grx2 from two different human cell lines suggested the presence of the cluster *in vivo*. Because only apo-Grx2 is enzymatically active, the cluster was proposed to serve as redox sensor for the activation of the protein during conditions of oxidative stress (27). Two recent studies demonstrated that the iron–sulfur cluster is complexed by the two N-terminal active site thiols of two Grx2 monomers and two molecules of GSH. The two molecules of GSH are bound noncovalently to the proteins and, *in vitro*, in equilibrium with GSH in solution (4, 18). This unusual holo-Grx2 complex may be the basis for the activation of Grx2 upon changes in the cellular redox state. In this model, the holo-Grx2 complex dissociates yielding enzymatically active Grx2, when GSH becomes the limiting factor for cluster coordination. When the active site of human Grx1 (Cys–Pro–Tyr–Cys), which normally cannot bind the cluster, is changed to the corresponding Cys–Ser–Tyr–Cys sequence of Grx2, Grx1 becomes able to complex a [2Fe-2S] cluster as well (4).

To our knowledge, no study has yet addressed the expression of nonmitochondrial Grx2 isoforms in humans. This lack of direct experimental evidence prompted us to screen various tissues and transformed cells for various Grx2 transcript variants. Our results demonstrate the production of mRNAs corresponding to different Grx2 transcript variants. The transcript variant encoding mitochondrial Grx2a was found ubiquitously, whereas Grx2b transcripts could only be detected in testis and transformed cells. Moreover, we have discovered a third, also testis/cancer-specific, mRNA variant, originated from alternative splicing of the Grx2b encoding pre-mRNA.

MATERIALS AND METHODS

General methods

Chemicals were of analytical grade or better and, unless otherwise stated, purchased from Sigma (St. Louis, MO). Materials for molecular biology were purchased from MBI Fermentas (St. Leon-Rot, Germany). Plasmid DNA was purified from bacteria using the Mini and Midiprep Kit from Qiagen (Hilden, Germany). SDS-PAGE was run using the Novex Mini-Cell and precasted NuPAGE gels (12% acrylamide, Bis-Tris, Invitrogen, Carlsbad, CA), according to the manufacturer's instructions.

Cell culturing

The cell lines investigated, summarized in Table 1, were cultivated in either DMEM ($1\ g \cdot l^{-1}$) or RPMI 1640 medium supplemented with 10% heat-inactivated fetal calf serum, 2 m*M* glutamine, and 100 U/ml penicillin and streptomycin mix (PAA, Cölbe, Germany) at 37°C in 90% humidified atmosphere containing 5% CO_2. To test the expression of Grx2 transcript variants upon hypoxia, HeLa and HEK293 cells were cultivated in DMEM (1 and $4.5\ g \cdot l^{-1}$ D-glucose, respectively) at 1% oxygen for 0 (control), 24, 48, or 72 h, whereupon they were trypsinized and harvested.

RNA and cDNA preparation

5×10^6 to 10^7 cells from different cell lines were harvested during the log phase of the culture. The cells were washed twice with PBS, scraped off the plate, resuspended in 10 ml PBS, and collected by centrifugation at 1,000 rpm for 5 min. The pellet was resuspended in 100 μl PBS + 600 μl RNase Later (Ambion, Austin, TX) RNA stabilizing reagent. Total RNA from these cells was prepared using the RNeasy Mini Kit (Qiagen), following the supplied instructions. First strand cDNA was synthesized from 3 μg total RNA using the RevertAid H minus First Strand cDNA synthesis Kit (MBI Fermentas) and oligo-dT primer. For the analysis of Grx2 mRNA isoforms in nonmalignant human tissue, normalized human multiple tissue cDNA panels (I and II) were purchased from Clontech (Mountain View, CA).

Table 1. Cell Lines Analyzed in This Study

Name	*Origin*
A549	Non-small cell lung carcinoma
BL28	Burkitt's lymphoma
BL30	Burkitt's lymphoma
BL41	Burkitt's lymphoma
D238	Medulloblastoma
D324	Medulloblastoma
DFSK-1	Medulloblastoma
H23	Lung cell carcinoma
H157	Non-small cell lung carcinoma
HCC1937	Breast cancer
HeLa	Cervix tumor
IARC-139	EBV-transformed lymphocytes (derived from the same patient as BL28)
IARC-171	EBV-transformed lymphocytes (derived from the same patient as BL41)
IMR-32	Medulloblastoma
Jurkat	Acute T cell leukemia
RAMOS	Burkitt's lymphoma
SH-SY-5Y	Neuroblastoma
SK-N-AS	Neuroblastoma
SK-N-BE(2)	Neuroblastoma
SK-N-DZ	Neuroblastoma
SK-N-F1	Neuroblastoma
SK-N-SH	Neuroblastoma
U1285	Small cell lung carcinoma
U1810	Non-small cell lung carcinoma

Polymerase chain reaction

PCR reactions were performed in programmable thermocyclers from Biometra (Göttingen, Germany) and MJ Research (Biorad, Hercules, CA) in a total volume of 20 μl containing 200 μM dNTPs, 1.5 mM Mg^{2+}, ~4 ng template cDNA, 0.5 μM of each primer, and 1.25 U recombinant Taq Polymerase (MBI Fermentas). The template was denatured at 95°C for 2 min and the following program was repeated 34 times: 95°C for 30 s, 54/60°C for 45 s, 72°C for 40 s. A final elongation step was performed at 72°C for 10 min. The oligonucleotides specific for the glyceraldehyde-3-phosphate dehydrogenase (G3PDH) control were included in the cDNA panels. Grx2 complementary oligonucleotides and further reaction conditions are listed in Table 2. PCR reactions were analyzed on 1.5–2% agarose gels (120 ml Tris-acetate-EDTA buffer, 14.5 × 19 cm).

Sequencing of PCR fragments

PCR products from agarose gels were extracted using Qiagen's Gel Extraction Kit and directly ligated into the pGEM-T vector (Promega, Madison, WI). Plasmids were sequenced from both 5′ and 3′ directions by the sequencing core facility at Karolinska Institutet, KISeq.

Subcellular localization of GFP fusion proteins

The cDNAs encoding Grx2a, Grx2b, and Grx2c were amplified by PCR and cloned into the EcoRI and BamHI sites of both vector pEGFP-N1 and vector pEGFP-C2 (Clontech) that allow the expression of C- and N-terminal GFP fusion proteins in mammalian cells, respectively.

HeLa cells were grown on coverslips in 24-well-plates. Prior to transfection using Exgene 500 (MBI Fermentas), mitochondria were stained with 1 μg/ml Mito Tracker Red 580 (Invitrogen, Carlsbad, CA). Cell nuclei were counterstained with Hoechst 33342 (1 μg/ml). The cells were mounted in PBS containing 90% glycerol and analyzed with a Zeiss 510 META confocal laser scanning microscope equipped with an inverted Zeiss Axiovert 200 microscope with a 63 × oil immersion objective (Zeiss, Oberkochen, Germany). Mix dyes were acquired by sequential multiple channel fluorescence scanning to avoid

Table 2. Oligonucleotides and Polymerase Chain Reactions

Oligonucleotides Used for RT-PCR

Name	*Target exon*	*Size*	*Sequence (5′ to 3′)*	*Position in cDNA*
PR096	Ia	28	CTGGTTTGGAGCAGGAGCGGCTCGGCAG	+37 to +64
PR107b	Ib	26	CCTCATGCACTGCTTCCAAGTGCCTG	−72 to −52
PR098	II	27	GAGAATTTAGCGACGGCGCCTGTGAAC	+28 to +54
PR099	IV rev	29	GTGAAGCCTATGAGTGTCAGTTGCACCTC	+303 to +275
PR100	IV-UTR rev	26	CATCTTCTTCGAGAAGACAATGCATG	+497 to +472

RT-PCRs

Oligonucleotides	*Target sequence*	*Expected length*	*Annealing temperature (°C)*
G3PDH primermix	G3PDH (control)	983	55
PR98/PR100	Exon II-IV UTR rev	477	54
PR96/PR99	Exon Ia-IVrev	353	60
PR107/PR99	Exon Ib-IVrev	477	60

For all oligonucleotides, complementary bases are printed in uppercase, noncomplementary in lowercase.

bleedthrough. Images were processed and colocalization was affirmed using Zeiss Software (LSM 510 Meta).

Protein expression and purification

The Grx2 cDNAs were amplified by PCR adding NdeI and BamH1 sites to the forward and reverse primers, respectively, and cloned into vector pET15b (Novagen, Darmstadt, Germany). PR137 (Grx2c fwd.): CACACACATATGGAGAGCAATACAATCATCATC, PR131 (Grx2b fwd.): CACACACATATGAACCCTCGAGATAAGCAAG, PR138 (Grx2 rev.): CACACAGGATCCTCACTGAAATTCTTTCCTCTTAC. Grx2 was expressed and purified as described previously (27). Since expression of Grx2b did not yield soluble protein, we used a modified protocol for *in vitro* refolding of inclusion body proteins (39). Cells were disrupted by a combination of lysozyme treatment and sonication. The crude extract was centrifuged at 20,000 *g* for 30 min. The pellet containing inclusion bodies was resuspended in 50 m*M* sodium phosphate buffer, pH 8, 300 m*M* NaCl, and 1 % Triton-X100 and centrifuged at 12,000 *g* for 30 min. The pellet was resuspended in 50 m*M* sodium phosphate buffer, pH 8, containing 300 m*M* NaCl, and centrifuged again. Next, the pellet was resuspended in 6 *M* guanidine HCl, 100 m*M* dithiotreitol, and 100 m*M* Tris/HCl, pH 8, and incubated during gentle shaking for 2 h at room temperature. The solution was centrifuged at 20,000 *g* for 30 min. Dithiotreitol was removed from the supernatant using prepacked Sephadex G-25 gelfitration columns (Amersham, Upsalla, Sweden) equilibrated with 6 *M* guanidine HCl, and 100 m*M* Tris/HCl, pH 8. The protein was purified by immobilized metal affinity chromatography using Talon (Novagen). Unspecific bound protein was removed by two wash steps with 50 m*M* sodium phosphate, pH 8, 300 m*M* NaCl, 6 *M* guanidine HCl, and the same buffer containing 50 m*M* imidazole. The protein was eluted in the washing buffer containing 300 m*M* imidazole. The pure protein was gently refolded by dialysis (MWCO: 6–8 kDa, Spectrum) against 200 ml washing buffer and, over a period of 20 h, slowly increasing amounts of 2 l of 50 m*M* sodium phosphate buffer, pH 8, 300 m*M* NaCl at 4°C. Residual guanidine and imidazole were removed using Sephadex G25 columns equilibrated with the dilution buffer.

[Fe,S] cluster reconstitution

Iron–sulfur cluster reconstitution was performed as described in detail in reference (4).

Spectroscopy

UV-VIS spectra were recorded with a Shimadzu (Kyoto, Japan) UV-2100 two beam spectrophotometer. Circular dichroism (CD) spectra were recorded using an Aviv (Lakewood, NJ) 202SF spectropolarimeter with a 1 mm path-length sealed cuvette at 25°C and a scan rate of 1 nm min^{-1}. Reference spectra were subtracted from the average of four spectra recorded over a range of 190–260 nm using 7.4–15 μM protein in a buffer containing 5 m*M* potassium phosphate, pH 8, and 100 m*M* KCl.

Immunological detection of Grx2

Antisera against human Grx2 were raised against the common part of Grx2a and Grx2b (28). This common part is identical to Grx2c. The Grx2-specific ELISA was performed as described before (29). The standard curves were calculated by regression analysis applying a four-parameter logistic equation using Grace (http://plasmagate.weizmann.ac.il/Grace, last accessed November 20, 2007).

Proteins from polyacrylamide gels were transferred onto nitrocellulose membrane (BioRad) by wet transfer as suggested by the manufacturer (Invitrogen NuPage Mini-Cell). After blocking the membranes for 1 h at room temperature in phosphate-buffered saline (PBS, 137 m*M* NaCl, 3 m*M* KCl, 6.5 m*M* NaHPO, 1.5 m*M* KH_2PO_4) containing 0.5% Tween-20 and 5% nonfat dry milk powder (Semper, Stockholm, Sweden), rabbit anti-Grx2 antibodies, or $(NH_4)_2SO_4$-precipitated serum from an Grx2 immunized rabbit, were added to a final dilution of 1:2,000 and 1:1,000, respectively, and left to incubate at 4°C overnight. To prove the specificity of the serum, a negative control was used where the serum was pre-incubated for 1 h with 100 μg of pure Grx2. The antigen–antibody complexes were identified by incubation with biotin-coupled anti-rabbit antibodies (1:1,000, Dako, Glostrup, Denmark) for 1 h at room temperature in blocking buffer, followed by incubation of alkaline phosphatase-conjugated streptavidin (1:1,000) in PBS plus 0.5% Tween-20, 5% BSA, and 0.02% NaN_3. The antibody binding was visualized using NBT/BCIP (Roche, Mannheim, Germany).

For the identification of Grx2 isoforms by immunocytochemistry, cDNAs encoding the three different Grx2 isoforms were amplified by PCR and cloned into the NheI and BglII sites of vector pExpress (1). Prior to transfection of HeLa cells using Nanofectine as suggested by the manufacturer (PAA), cells were counter stained with 200 n*M* Mitotracker Deep Red 633. Twenty-four hours after transfection, cells were fixated with 4% paraformaldehyde (Merck, Darmstadt, Germany) for 30 min. Next, the cells were washed with PBS (3 times, 5 min) followed by permeabilization and blocking with blocking buffer (10 m*M* HEPES, 0.3% Triton X-100, 3% BSA) for 1 h. Subsequently, the samples were incubated with anti-Grx2 antibodies diluted 1:1,000 in blocking buffer over night at 4°C. Following three washing steps with PBS for 5 min, immunocomplexes were detected with Alexa 488-coupled anti-rabbit antibodies (Invitrogen). When indicated, nuclei were counterstained with 1 ng/μl Hoechst 33342 (Sigma). Images were recorded with a Leica TCS SP2 confocal laser scanning microscope using a 40× oil planapochromat lens (Leica, Heidelberg, Germany). Deconvolution and analysis of co-localization was performed using the software package Huygens (Scientific Volume Imaging, Hilversum, The Netherlands).

Paraffin-embedded slides of human testis were purchased from ProSci Incorporated (Poway, CA). The sections were deparaffinized in xylene and rehydrated in ethanol to distilled water. Tissue was processed with the peroxidase–anti-peroxidase method as described in Ref. 6, with minor modifications. Briefly, endogenous peroxidase was blocked by incubating the sections for 30 min in PBS containing 1% H_2O_2. Following three times washing in PBS, the tissue was penetrated for 2.5 h using PBS containing 0.1% Triton X-100 (PBST). Next, the

sections were incubated for 40 h at 4°C in the presence of the Grx2 antibody (1:50). The samples were washed three times in PBST, and incubated with a biotinylated anti-rabbit antibody (1:200 Vector) in PBST for 1 h. Finally, the sections were incubated with 100 μl of an ABC-complex, washed two times with both PBS and 0.2 *M* acetate buffer, and developed with 0.035% 3.3¸-diaminobenzidine. Following 10 min wash in PBST and dehydration, sections were mounted and examined with a Zeiss Axiophot microscope. Adobe Photoshop 8.0—www.adobe.com (074122)—was used for processing and analyzing the images.

Enzymatic assays

Enzymatic activity of Grx with GSH as electron donor was determined using the HED assay (31), modified as described in Ref. 4. The reduction of GSSG by Grx2 with TrxR as electron donor was done according to Ref. 19, using 10 n*M* of TrxR and 100 μM GSSG as substrate. The activity was expressed in units per mg, one U corresponds to one μmol per min.

RESULTS

For the analysis of Grx2 mRNA variants, we have screened human tissues for the following fragments: (a) exons II, III, and IV, representing the common/core part of the human Grx2 variants, (b) exons Ia, II, III, and IV, encoding the mitochondrial isoform Grx2a, and (c) exons Ib, II, III, and IV, encoding the previously suggested Grx2b (28).

Grx2 mRNA isoforms in nonmalignant human tissue

Grx2 mRNA variants in nonmalignant human tissues were analyzed using commercially available normalized first strand cDNA from heart, brain, placenta, lung, liver, skeletal muscle, kidney, pancreas, spleen, thymus, prostate, testis, ovary, small intestine, colon, and leukocyte. Figure 1 shows representative pictures from the PCRs separated by gel electrophoresis. Pooled cDNA served as tissue-independent positive control.

First, we screened the different tissues for the common part of the expected Grx2 transcript variants, represented by exons II to IV. The presence of one band in each sample with only minor differences in intensity demonstrated that Grx2 mRNA was present in all tissues analyzed (Fig. 1, second panel), confirming previous findings (28). Similar results were obtained for the mitochondrial isoform (exons Ia, to IV); one band of the expected size (see Table 2) with small differences in intensity in all samples was observed (Fig. 1, third panel). In contrast, PCRs specific for the previously suggested second isoform (exons Ib. II, III, and IV) yielded products only in cDNA derived from testes (Fig. 1, bottom panel). Unexpectedly, the PCRs yielded two products. One band of the expected size of ~480 bp, and a second of ~380 bp. A representative EST clone that was used as positive control yielded only the expected reaction product of 480 bp.

Grx2 in transformed cells

Many cancer cells show alterations in expression levels of enzymes involved in oxidative stress response. We therefore screened a number of human cancer cell lines (see Table 1) derived from blood, breast, cervix, lung, and the nervous system. As before, we obtained nearly equally strong bands in our control reaction (exons II to IV) and in reactions specific for the mitochondrial isoform (exons Ia to IV, Fig. 2), supporting the idea that Grx2 may be highly expressed in cancer cells (28). In contrast to normal tissue, the testis-specific Grx2b isoform was detected in about two-thirds of all analyzed samples. Again, the reactions yielded two bands of ~380 and 480 bp. However, the ratio between these bands differed significantly among the cell lines. IARC139, BL30, DFSK-1, D283, HCC1937, A549, and HeLa cells yielded approx. equally strong signals for both fragments. BL28 cells contained mainly the smaller fragment, SK-N-F1, and SK-N-AS, D324, H23, and Jurkat cells gave rise mainly to the larger fragment. Testis and solid cancer tissue exhibit the lowest oxygen concentrations in the human body. To investigate the influence of these hypoxic conditions on the expression of Grx2 mRNA variants, we propagated HeLa and HEK293 cells at 1% oxygen for up to 72 h, however, we could not detect significant differences in expression pattern (data not shown).

A new third human Grx2 isoform

To investigate the nature of the two products obtained from the exon 1b-specific PCRs, we extracted and sequenced them

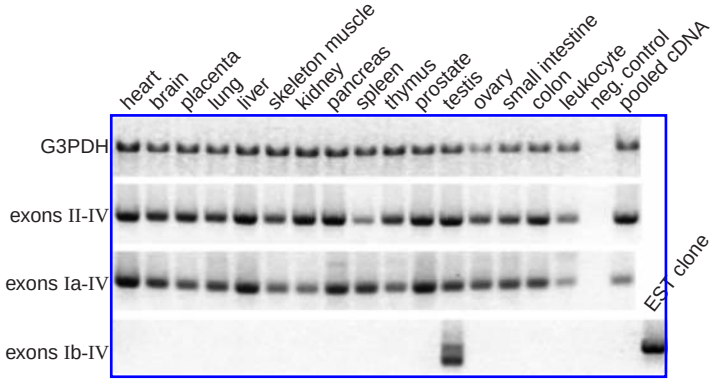

FIG. 1. RT-PCR screen for human Grx2 mRNA isoforms in various tissues. cDNAs from multiple tissue cDNA panels were used as templates. G3PDH and Grx2 exon II to IV fragments were amplified as controls. Pooled cDNA was used as tissue-independent control. The negative control contained water instead of template. A plasmid containing a full-length Grx2b EST clone was used as additional positive control for the exon Ib to exon IV-specific PCR.

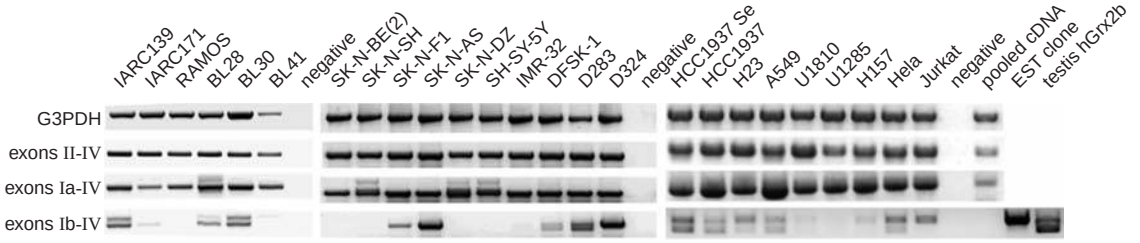

FIG. 2. RT-PCR screen for human Grx2 mRNA isoforms in cancer cell lines. cDNAs reversely transcribed from total RNA using oligo-dT primer were used as PCR templates. G3PDH and Grx2 exon II to IV fragments were amplified as controls. Pooled cDNA was used as independent control. The negative control contained water instead of template. A plasmid containing the full Grx2b EST clone and testis cDNA were used as positive controls for the exon Ib to exon IV-specific PCR. The origins of the different cell lines are listed in Table 1.

from both testis and several cell lines. All samples yielded the same results, depicted in Fig. 3, demonstrating that the two products were derived from alternative splicing events. Exon Ib contains two alternative splice donor sites (Fig. 3B). The previously suggested Grx2b isoform (*i.e.*, the 480 bp fragment) was derived from full-length exon Ib. An alternative splice donor site, located 101 bp upstream, gave raise to the 380 bp fragment. The longest possible open reading frame for this transcript variant ranges from the ATG at the beginning of exon II to the termination site in exon IV (Fig. 3), thus yielding a new isoform named Grx2c.

Subcellular localization of the isoforms

To confirm the subcellular localization of Grx2a in mitochondria (9, 28) and investigate the localization of Grx2b and Grx2c, we followed two independent strategies. First, we have expressed both N- and C-terminal GFP fusion proteins in HeLa cells (Fig. 4A). Our results confirm the mitochondrial localization of Grx2a mediated by an N-terminal transit peptide as seen from the mitochondrial staining of Grx2a-GFP transfected cells and the diffuse, unspecific staining of GFP-Grx2a transfected cells (Fig. 4A, 1st column). Unlike previously suggested (28), we could not confirm an exclusive nuclear or perinuclear staining of cells expressing Grx2b-GFP or GFP-Grx2b (Fig. 4A, 2nd column). Instead, expression of these proteins as well as expression of the corresponding Grx2c-GFP fusion proteins (Fig. 4A, 3rd column) led to a diffuse staining of the cells, indicating both cytosolic and nuclear localization of these proteins. Second, to rule out possible artifacts resulting from the GFP fusion protein, we transiently expressed the three Grx2 isoforms without GFP fusion at medium levels (approximately threefold overexpression when quantified by ELISA) and investigated the localization of the proteins in fixated cells by immunocytochemistry. The results, depicted in Fig. 4B, corroborate the results outlined above. Grx2a was identified in mitochondria, Grx2b and Grx2c were detected in both the cytosol and nucleus. This distribution did not change when the cells were stressed with hydrogen peroxide, cumene peroxide, or doxorubicin for different time points prior to fixation (not shown).

Characterization of Grx2b and Grx2c

With respect to primary structure, the newly discovered cytosolic isoform Grx2c is almost identical to processed mitochondrial Grx2a (28), that has been analyzed thoroughly biochemically and biophysically before. Grx2b contains an N-terminal extension. The fact that the subcellular distribution of Grx2b was not affected when the proteins were expressed as N- or C-terminal GFP fusion protein suggests that this exten-

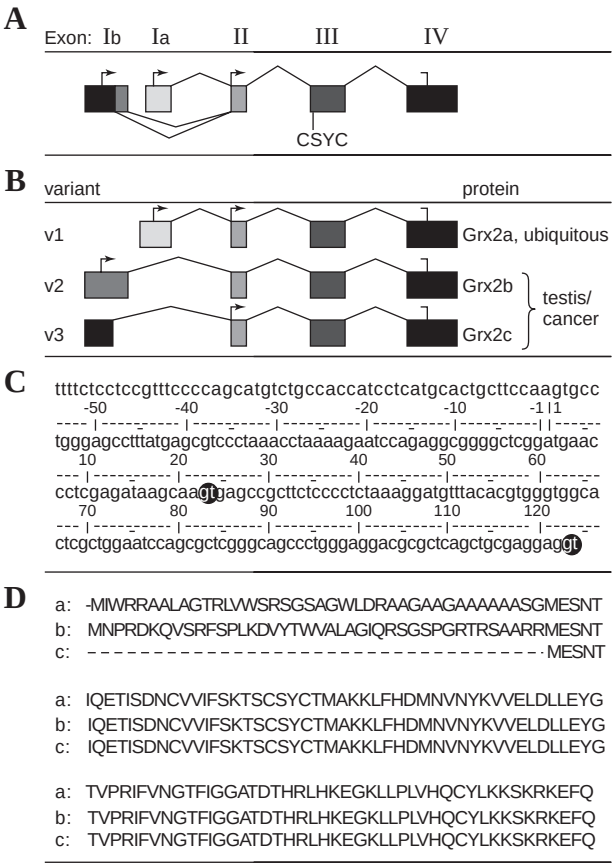

FIG. 3. Isoforms of human Grx2. (**A**) Alternative splicing and transcription initiation of human Grx2. The region encoding the active site is indicated (CSYC). (**B**) Transcript variants of human Grx2. The longest possible open reading frames are indicated by *arrows* and *ticks*. (**C**) Alternative splice donor sites in exon Ib, numbered according to the open reading frame of Grx2b, whose transcript variant is derived from the downstream GT splice donor site. The 101 bp upstream located alternative splice donor site is located in a different reading frame, in which no alternative start codon is present (only partially shown). (**D**) Primary sequence alignment of human Grx2 protein isoforms.

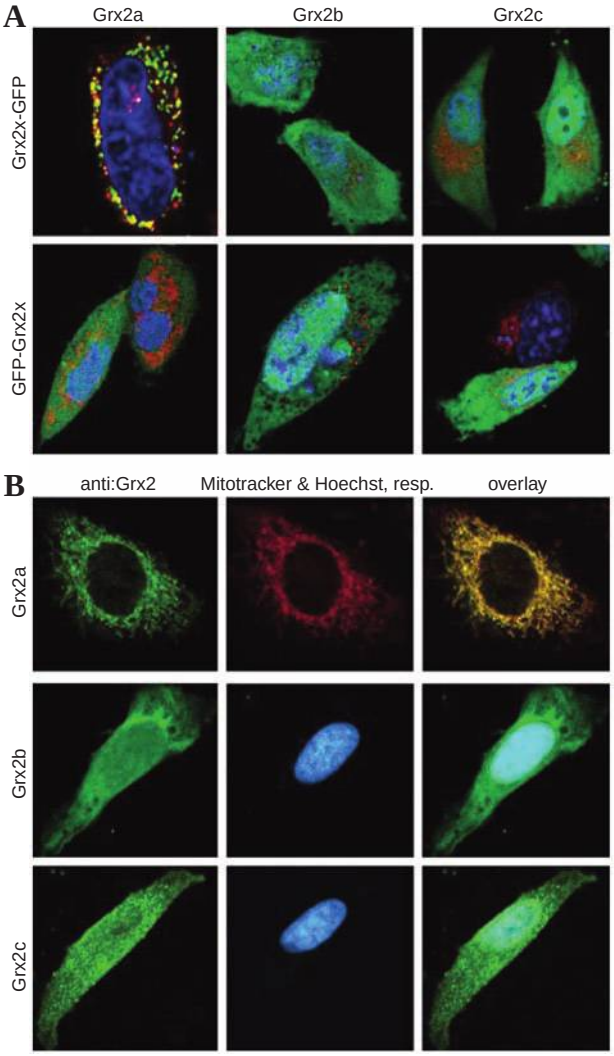

FIG. 4. Localization of Grx2 isoforms. (**A**) Confocal images of living HeLa cells transfected with plasmids for the expression of Grx2 GFP fusion proteins. C-terminal GFP fusion proteins with Grx2a, Grx2b, and Grx2c are displayed in the *upper panel*, N-terminal GFP fusions in the *lower panel*. Mitochondria and nuclei were counter stained using Mitotracker Red 580 (*red*) and Hoechst 33342 (*blue*), respectively. (**B**) Confocal images of fixated anti-Grx2 immunostained HeLa cells transfected with plasmids for the expression of Grx2a (*upper panel*), Grx2b (*middle panel*), and Grx2c (*lower panel*). Anti-Grx2 immunocomplexes were detected with secondary anti-rabbit immunoglobulines labeled with Alexa-488. Mitochondria were counterstained using Mitotracker Deep Red 633 (*red*), nuclei with Hoechst 33342 (*blue*). The *yellow color* is the result of an overlay between green and red fluorescence and confirms the mitochondrial localization of the Grx2a. Both experiments indicate a cytosolic and nuclear localization of Grx2b and Grx2c. For each picture, a representative image of the staining pattern is shown. Five distinct experiments were performed with essentially identical results.

sion does not function as signal peptide. This is in agreement with predictions from bioinformatics (not shown). Despite of multiple strategies, we were not able to express Grx2b in soluble form in *E. coli*. However, we were able to refold the protein *in vitro*. CD spectra recorded for refolded Grx2b and native Grx2c were almost identical (not shown). Moreover, when assayed for enzymatic activity using GSH as electron donor and the mixed disulfide between GSH and â-mercaptoethanol formed in the HED assay as substrate, refolded Grx2b exhibited essentially the same specific activity as Grx2c (*i.e.*, 16.2 ± 4.8 and 16.9 ± 4.1 U mg^{-1}, respectively). With TrxR as electron donor, Grx2b reduced GSSG with a specific activity of 15.3 ± 3.3 compared to 29.7 ± 3.5 mU mg^{-1} determined for Grx2c. This value for Grx2c did not change significantly when the protein was objected to the denaturation/refolding procedure applied to Grx2b.

We next analyzed the ability of Grx2b to form the iron–sulfur cluster-bridged dimer using the recently established *in vitro* reconstitution assay (4). As depicted in Fig. 5, Grx2c, but not the refolded Grx2b, was able to form the holo-complex. Iron–sulfur cluster biosynthesis is dependent on mitochondria, but can take place in the cytosol as well (24). Thus, both cytosolic and nuclear Grx2 may harbor an iron–sulfur cluster *in vivo*.

Identification of Grx2 protein isoforms

To investigate how well the antigen-purified antibodies raised against Grx2 (29) may recognize both folded and denatured Grx2b, we analyzed the protein by ELISA and Western blotting. In ELISA, Grx2b reacts with about fivefold lower sensitivity compared to Grx2c (Fig. 6A). In Western blotting, no significant difference in sensitivity was seen between the isoforms (±11%, Fig. 6B). However, the sensitivity in general was too low to identify Grx2 in cellular extracts. To overcome this problem, serum was used instead of affinity purified antibodies. This way, we were able to obtain three weak but specific signals in HeLa extracts of approx. 14.5, 15, and 18 kDa (Fig. 6C). These bands correspond well to the calculated molecular weights of Grx2c (14.1 kDa), processed Grx2a (15 kDa), and Grx2b (18.8 kDa).

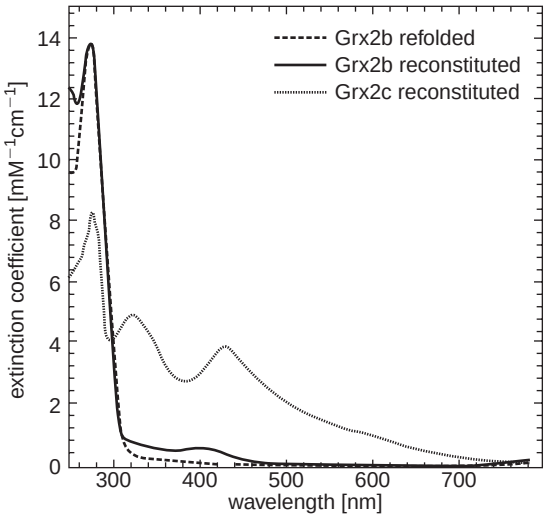

FIG. 5. Iron–sulfur cluster coordination by Grx2b and Grx2c. UV-Vis spectra of Grx2b before reconstitution (*dashed line*), Grx2b after reconstitution (*straight line*), and Grx2c after reconstitution (*dotted line*). Enzymatically active protein was subjected to a recently developed reconstitution assay (4). Only Grx2c was able to complex the [2Fe–2S] cluster.

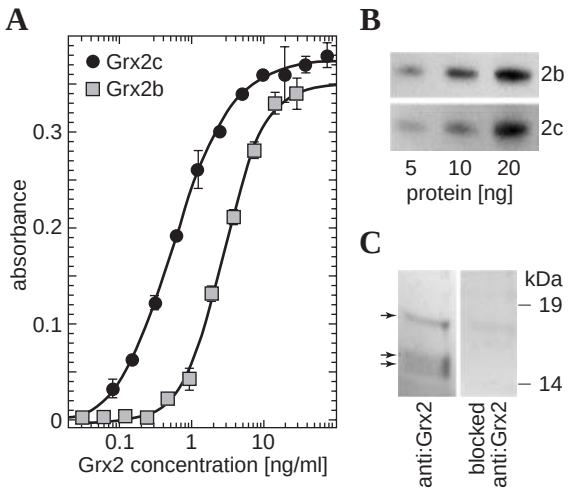

FIG. 6. Immunological detection of Grx2b and Grx2c. (**A**) ELISA standard curves for Grx2b (*gray squares*) and Grx2c (*black circles*). (**B**) Western blot of purified Grx2b (*upper panel*) and Grx2c (*lower panel*) using antigen-purified antibodies. (**C**) Western blot of HeLa extracts (70 μg/lane) using anti-Grx2 serum (*left lane*) and anti-Grx2 serum pre-incubated with 100 μg Grx2 for 1 h at room temperature (*right lane*). The lack of significant signals in the control strongly suggest that the three detected bands (*see arrows*) correspond to the three Grx2 isoforms: Grx2c (14.1 kDa), processed Grx2a (15 kDa), and Grx2b (18.8 kDa).

To shed some light on possible functions of Grx2 in human testicles, we studied the distribution of Grx2 in the different cell types of the testicle (Fig. 7). Grx2 immunolabeling resulted in a more consistent and strong staining in spermatids [*i.e.*, in both round (RS) and elongated spermatids (ES)]. Specific Grx2 staining was also observed in spermatogonia (SP) and Sertoli cells (SER). In general, the labeling increased during spermatid development and appeared to be concentrated in the cytoplasm.

DISCUSSION

Alternative splicing and transcription initiation mechanisms greatly increase the number of functionally different proteins transcribed from a particular gene. Multiple transcript variants were proposed for both human and mouse Grx2, however, so far only one transcript variant encoding the mitochondrial isoform of mammalian Grx2 (Grx2a) has been demonstrated experimentally (10, 21, 28). Here, we have identified and confirmed two additional transcript variants of human Grx2 whose expression is restricted to testicular tissue and transformed cells.

Mitochondrial Grx2a, and its supposedly cytosolic/nuclear siblings Grx2b and Grx2c, share the same Grx core domain encoded by exons II, III, and IV of the GLRX2 gene (Fig. 3d). Grx2a, once it has been processed during mitochondrial translocation, and Grx2c are essentially the same protein. They can both receive electrons from GSH as well as TrxR *in vitro* and they can both complex the regulatory iron–sulfur cluster. Grx2b, on the other hand, may be constitutively active or regulated by other mechanisms, since the protein cannot form the dimeric holo-complex. This finding may be caused by a lack of structural integrity of the refolded Grx2b protein, however, it may as well indicate a different accessibility of the active site for protein–protein interactions, that could interfere with dimerization. This assumption is supported by the decreased activity of Grx2b with TrxR. The physiological functions of reduction by TrxR and the iron–sulfur cluster complexes remain to be established.

Grx2b has previously been suggested to be a nuclear protein, based on the observation that HeLa cells expressing a Grx2b–GFP fusion protein showed a dotted fluorescence pattern located predominantly in the perinuclear area. A positive stretch of amino acids in the C-terminus of the protein was suggested to constitute a nuclear localization signal (28). In our hands, the cells expressing neither Grx2b-GFP nor the GFP–Grx2b exhibited this pattern. Instead, we have seen a diffuse cytosolic and nuclear localization. To rule out artifacts induced by the GFP fusion partner and the fixation procedure, we have also analyzed HeLa cells recombinantly expressing the three (tag-free) Grx2 isoforms at medium levels by immunocytochemistry. These experiments yielded essentially the same distribution of the three isoforms as described above. What else could be the reason for this significant difference to the previous study? Notably, the article by Lundberg *et al*. (28) does not show nuclear staining for Grx2b in HeLa cells, but an immunological detection of Grxb in nuclear extracts from Jurkat

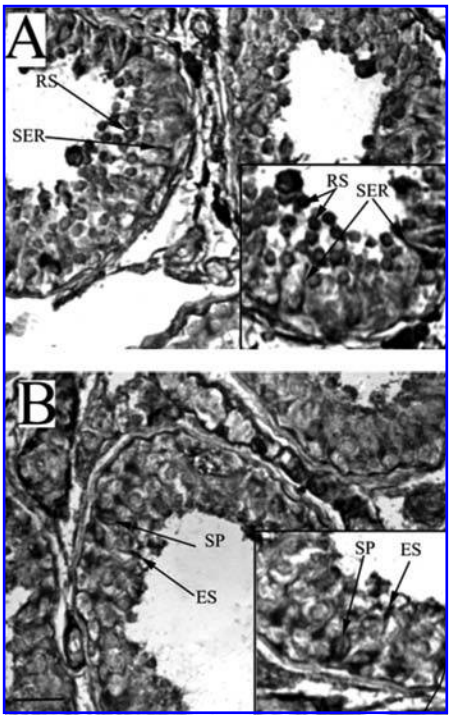

FIG. 7. Localization of Grx2 in human testicles. Light microscopic localization of Grx2 revealed by immunoperoxidase staining with anti-Grx2 antibodies raised against the common part of all Grx2 isoforms. Intense staining of Grx2 immunostaining was found in the cytoplasm of elongated spermatids. Insets in (**A**) and (**B**) are magnifications and reveal more details of the Grx2-specific staining. Bar, 50 μm.

T-cells. This may point to different subcellular distributions in different cell types. A second possible explanation could be a dynamic distribution of Grx2b and maybe even Grx2c between cytosol and nucleus. However, we could not detect any changes in subcellular distribution when the cells were objected to oxidative stress prior to analysis. Further studies will address this question.

Alternative transcript variants have also been reported for other members of the mammalian Trx family of proteins. Three splice variants of cytosolic Trx1 lacking exon III, exons II and III, and the poly A-tail, respectively, have been described (3, 13, 17). Two Grx1 variants have been described that differ in the 3′ untranslated regions but share the same open reading frame (34). An intriguingly complex transcription and splicing pattern has been revealed for cytosolic TrxR1 (33, 40, 46). Remarkably, one of these transcript variants contains a glutaredoxin domain fused to the N-terminus of TrxR1 and is, as various other N-terminal TrxR1 variants, primarily expressed in testes (46). In a strikingly similar manner, the homologous thioredoxin-glutathione reductase (TGR) is composed of an N-terminal Grx domain and a C-terminal TrxR domain and is predominantly expressed in testes, particularly in elongated spermatids (47). Another seleno-oxidoreductase worth mentioning is phospholipid hydroperoxide reductase (PHGPx). This GSH peroxidase is, by means of alternative splicing, expressed in three isoforms: the ubiquitously present cytosolic form and two testis-specific isoforms targeted to mitochondria and the nucleus, respectively (22, 35, 36, 42). PHGPx exists as soluble enzyme in spermatids but persists in mature sperm as structural, insoluble, oxidatively cross-linked protein representing the major component of the mitochondrial midpiece capsule (50). It was proposed that TGR and PHGPx together serve as a disulfide bond formation system during spermatogenesis (47). Furthermore, testicular cells are equipped with a series of tissues-specific members of the Trx family of proteins (32).

What could be the functions of Grx2b and Grx2c in testis and transformed cells? The restriction to testis may well reflect the special redox requirements of this organ. Spermatogenesis is a highly complex process of cellular differentiation, and oxidative crosslinking of proteins by means of specific disulfide linkages plays an important role in sperm maturation (43, 48). In this respect, nonmitochondrial Grx2 may act as disulfide isomerase in different compartments, a possible function that has been previously described for Grxs (41, 52). This assumption is also consistent with the increase in Grx2 immunostaining during spermatid development.

Many genes predominantly expressed in testis and malignancies have suggested functions in cell cycle regulation, transcriptional control, or cell survival (53). In HeLa cells, Grx2 plays a major role in cell survival upon treatment of the cells with oxidative stress-inducing apoptotic agents (26). Overexpression of both mitochondrial Grx2a and of a cytosolic mutant (identical to Grx2c identified here) provided protection from apoptosis induced by the anti-cancer agents doxorubicin/adriamycin and 2-deoxy-D-glucose. The protection by cytosolic Grx2 was less efficient, especially after treatment with 2-deoxy-D-glucose (8). The ubiquitous expression of Grx2a may thus reflect the general importance of this isoform in maintenance of mitochondrial redox homeostasis. The apparent restricted expression of the supposedly cytosolic/nuclear Grx2 isoforms may be consistent with functions in cellular differentiation and transformation.

RNR can use electrons from both Trxs and Grxs for the supply of DNA synthesis with deoxynucleotides (14, 23). In mammalian cells, however, the importance of these proteins as electron donor is not well understood, because the tissue distribution of these redoxins is not related to cell proliferation or DNA synthesis (37). One might therefore speculate about a function of cytosolic Grx2 as electron donor for RNR in the highly proliferative spermatogonia cells that contain both RNR and Grx2 but neither Trx1 nor Grx1 (12, 38). More research is required to analyze this possibility.

DNA methylation is the main mechanism controlling the expression of testis/cancer-associated genes (53). This epigenetic regulation is based on the methylation of cytosines in so-called CpG islands (20). These regions are often located in the 5′ regulatory sequences of genes (7). Could this be the mechanism regulating the expression of Grx2 isoforms? In support of this hypothesis, the human GLRX2 gene contains two potential CpG islands in its 5′ region. The first one is located directly upstream of exon Ib and covers the potential promotor of Grx2b and Grx2c (length = 232 bp, %GC = 60.7, obs/exp CpG = 0.7). The second one covers exon Ia and the predicted promotor of the Grx2a isoform (length = 720 bp, %GC = 67.3, obs/exp CpG = 0.88).

In conclusion, we have demonstrated the ubiquitous expression of Grx2's mitochondrial isoform (Grx2a) in human tissues. We have confirmed and identified two alternative transcript variants expressed exclusively in testis and transformed cells that encode cytosolic/nuclear proteins. Our results provide evidence for the expression of the proteins corresponding to these transcripts *in vivo*. Together, the results presented here provide the first evidence for potential roles of Grx2 in cellular differentiation and tumor progression.

ACKNOWLEDGMENTS

The authors wish to thank Drs. Boris Zhivotovski, Bertrand Joseph, and Ralf Jacob for cell lines and help with confocal microscopy, Drs. Per Kogner, John–Inge Johnsen, Laura Papp, and Javier Avilo–Cariño for cell lines, Drs. Marcus Conrad and Antonio Miranda–Vizuete for helpful discussions, Arvind Viswanathan for reading the manuscript, and Lena Ringden for excellent administrative assistance. This study was supported by grants from ANPCyT PICT 15001, the Deutsche Forschungsgemeinschaft, Karolinska Institutet, the Swedish Cancer Society, and the Swedish Society for Medical Research.

ABBREVIATIONS

ES, elongated spermatids; Grx, glutaredoxin; GSH, (reduced) glutathione; GSSG, glutathione disulfide; PHGPx, phospholipid hydroperoxide reductase; RNR, ribonucleotide reductase; ROS, reactive oxygen species; RS, round spermatids; Ser, Sertoli cells; SP, spermatogonia; TGR, thioredoxin and glutathione reductase; Trx, thioredoxin; TrxR, thioredoxin reductase.

REFERENCES

1. Arakawa H, Lodygin D, and Bhuerstedde JM. Mutant loxP vectors for selectable marker recycle and conditional knock outs. *BMC Biotechnol* 1: 7, 2001.
2. Beer SM, Taylor ER, Brown SE, Dahm CC, Costa NJ, Runswick MJ, and Murphy MP. Glutaredoxin 2 catalyses the reversible oxidation and glutathionylation of mitochondrial membrane thiol proteins. *J Biol Chem* 279: 47939–47951, 2004.
3. Berggren MM and Powis G. Alternative splicing is associated with decreased expression of the redox proto-oncogene thioredoxin-1 in human cancers. *Arch Biochem Biophys* 389: 144–149, 2001.
4. Berndt C, Hudemann C, Hanschmann EM, Axelsson R, Holmgren A, and Lillig CH. How does iron-sulfur cluster coordination regulate the activity of human glutaredoxin 2? *Antioxid Redox Signal* 9: 151–157, 2007.
5. Bushweller JH, Åslund F, Wüthrich K, and Holmgren A. Structural and functional characterization of the mutant *Escherichia coli* glutaredoxin, C14S and its mixed disulfide with glutathione. *Biochemistry* 31: 9288–9293, 1992.
6. Capani F, Loidl F, Lopez–Costa JJ, Selvin–Testa A, and Saavedra JP. Ultrastructural changes in nitric oxide synthase immunoreactivity in the brain of rats subjected to perinatal asphyxia: neuroprotective effects of cold treatment. *Brain Res* 775: 11–23, 1997.
7. de Smet C, Lurquin C, Lethe B, Mertelange V, and Boon T. DNA methylation is the primary silencing mechanism for a set of germ line- and tumor-specific genes with a CpG-rich promotor. *Mol Cell Biol* 57: 3223–3229, 1999.
8. Enoksson M, Fernandes AP, Prast S, Lillig CH, Holmgren A, and Orrenius S. Overexpression of glutaredoxin 2 attenuates apoptosis by preventing cytochrome c release. *Biochem Biophys Res Commun* 327: 774–779, 2005.
9. Ghezzi P. Regulation of protein function by glutathionylation. *Free Radic Res* 39: 573–580, 2005.
10. Gladyshev VN, Liu A, Novoselov SV, Krysan K, Sun QA, Kryukov VM, Kryukov GV, and Lou MF. Identification and characterization of a new mammalian glutaredoxin, thioltransferase, GRX2. *J Biol Chem* 276: 30374–30380, 2001.
11. Gravina SA and Mieyal JJ. Thioltransferase is a specific glutathionyl mixed disulfide oxidoreductase. *Biochemistry* 32: 3368–3376, 1993.
12. Hansson HA, Rozell B, Stemme S, Engström Y, Thelander L, and Holmgren A. Different cellular distribution of thioredoxin and subunit M1 of ribonucleotide reductase in rat tissues. *Exp Cell Res* 163: 363–369, 1986.
13. Hariharan J, Hebbar P, Ranie J, Philomena, Sinha AM, and Datta S. Alternative forms of the human thioredoxin mRNA: identification and characterization. *Gene* 173: 265–270, 1996.
14. Holmgren A. Hydrogen donor system for *Escherichia coli* ribonucleoside-diphosphate reductase dependent upon glutathione. *Proc Natl Acad Sci USA* 73: 2275–2279, 1976.
15. Holmgren A. Glutathione-dependent synthesis of deoxyribonucleotides. Characterisation of the enzymatic mechanism of *Escherichia coli* glutaredoxin. *J Biol Chem* 254: 3672–3678, 1979.
16. Hurd TR, Costa NJ, Dahm CC, Beer SM, Brown SE, Filipovska A, and Murphy MP. Glutathionylation of mitochondrial proteins. *Antioxid Redox Signal* 7: 999–1010, 2005.
17. Jimenez A and Miranda–Vizuete A. Purification and characterization of delta3Trx-1, a splicing variant of human thioredoxin-1 lacking exon 3. *Protein Expr Purif* 27: 319–324, 2003.
18. Johansson C, Kavanagh KL, Gileadi O, and Oppermann U. Reversible sequestration of active site cysteines in a 2FE2S-bridged dimer provides a mechanism for glutaredoxin 2 regulation in human mitochondria. *J Biol Chem* 282: 3077–3082, 2007.
19. Johansson C, Lillig CH, and Holmgren A. Human mitochondrial glutaredoxin reduces S-glutathionylated proteins with high affinity accepting electrons from either glutathione or thioredoxin reductase. *J Biol Chem* 279: 7537–7543, 2004.
20. Jones PA. The DNA methylation paradox. *Trends Genet* 15: 34–37, 1999.
21. Jurado J, Prieto–Alamo MJ, Madrid–Risquez J, and Pueyo C. Absolute gene expression patterns of thioredoxin and glutaredoxin redox systems in mouse. *J Biol Chem* 278: 45546–45554, 2003.
22. Kelner MJ and Montoya MA. Structural organization of the human selenium-dependent phospholipid hydroperoxide glutathione peroxidase gene, GPX4: chromosomal localization to 19p13.3. *Biochem Biophys Res Commun* 249: 53–55, 1998.
23. Laurent TC, Moore EC, and Reichard P. Enzymatic synthesis of deoxyribonucleotides. IV. Isolation and characterization of thioredoxin, the hydrogen donor from *Escherichia coli. J Biol Chem* 239: 3436–3444, 1964.
24. Lill R and Mühlenhoff U. Iron-sulfur protein biogenesis in eukaryotes: components and mechanisms. *Annu Rev Cell Dev Biol* 22: 457–486, 2006.
25. Lillig CH and Holmgren A. Thioredoxin and related molecules—from biology to health and disease. *Antioxid Redox Signal* 9: 25–47, 2007.
26. Lillig CH, Lönn ME, Enoksson M, Fernandes AP, and Holmgren A. Short interfering RNA-mediated silencing of glutaredoxin 2 increases the sensitivity of HeLa cells towards doxorubicin and phenylarsine oxide. *Proc Natl Acad Sci USA* 101: 13227–13232, 2004.
27. Lillig CH, Berndt C, Vergnolle O, Lönn ME, Hudemann C, Bill E, and Holmgren A. Characterization of human glutaredoxin 2 as iron-sulfur protein: a possible role as redox sensor. *Proc Natl Acad Sci USA* 102: 8168–8173, 2005.
28. Lundberg M, Johansson C, Chandra J, Enoksson M, Jacobsson G, Ljung J, Johansson M, and Holmgren A. Cloning and expression of a novel human glutaredoxin, GRX2 with mitochondrial and nuclear isoforms. *J Biol Chem* 276: 26269–26275, 2001.
29. Lundberg M, Fernandes AP, Kumar S, and Holmgren A. Cellular and plasma levels of human glutaredoxin 1 and 2 detected by sensitive ELISA systems. *Biochem Biophys Res Commun* 319: 801–809, 2004.
30. Lundstrom–Ljung J and Holmgren A. Glutaredoxin accelerates glutathione-dependent folding of reduced ribonuclease A together with protein disulfide-isomerase. *J Biol Chem* 270: 7822–7828, 1995.
31. Luthman M and Holmgren A. Glutaredoxin from calf thymus. Purification to homogeneity. *J Biol Chem* 257: 6686–6689, 1982.
32. Miranda–Vizuete A, Sadek CM, Jimenez A, Krause WJ, Sutovsky P, and Oko R. The mammalian testis-specific thioredoxin system. *Antioxid Redox Signal* 6: 25–40, 2004.
33. Osborne SA and Tonissen KF. Genomic organisation and alternative splicing of mouse and human thioredoxin reductase 1 genes. *BMC Genomics* 2: 10, 2001.
34. Park JB and Levine M. Cloning, sequencing, and characterization of alternatively spliced glutaredoxin 1 cDNA and its genomic gene: chromosomal localization, mRNA stability, and origin of pseudogenes. *J Biol Chem* 280: 10427–10434, 2005.
35. Pfeifer H, Conrad M, Roethlein D, Kyriakopouluos A, Brielmeier M, Bornkamm GW, and Behne D. Identification of a specific sperm nuclei selenoenzyme necessary for protamine thiol cross-linking during sperm maturation. *FASEB J* 15: 1236–1238, 2001.
36. Roveri A, Maiorino M, Nissi C, and Ursini F. Purification and characterization of phospholipid hydroperoxide glutathione peroxidase from rat testis mitochondrial membranes. *Biochim Biophys Acta* 1208: 211–221, 1994.
37. Rozell B, Hansson HA, Luthman M, and Holmgren A. Immunohistochemical localization of thioredoxin and thioredoxin reductase in adult rats. *Eur J Cell Biol* 38: 79–86, 1985.
38. Rozell B, Barcena JA, Martinez–Galisteo E, Padilla CA, and Holmgren, A. Immunochemical characterization and tissue distribution of glutaredoxin, thioltransferase from calf. *Eur J Cell Biol* 62: 314–323, 1993.
39. Rudolph R and Lilie H. *In vitro* folding of inclusion body proteins. *FASEB J* 10: 49–56, 1996.
40. Rundlöf AK, Janard M, Miranda–Vizuete A, and Arnér ES. Evidence for intriguingly complex transcription of human thioredoxin reductase 1. *Free Radic Biol Med* 36: 641–656, 2004.
41. Ruoppolo M, Lundstrom–Ljung J, Talamo F, Pucci P, and Marino G. Effect of glutaredoxin and protein disulfide isomerase on the glutathione-dependent folding of ribonuclease A. *Biochemistry* 36: 12259–12267, 1997.
42. Schneider M, Vogt Weisenhorn DM, Seiler A, Bornkamm GW, Brielmeier M, and Conrad M. Embryonic expression profile of

phospholipid hydroperoxide glutathione peroxidase. *Gene Expr Patterns* 6: 489–494, 2006.
43. Shalgi R, Seligman J, and Kosower NS. Dynamics of the thiol status of rat spermatozoa during maturation: analysis with the fluorescent labeling agent monobromobimane. *Biol Reprod* 40: 1037–1045, 1989.
44. Shelton MD, Chock PB, and Mieyal JJ. Glutaredoxin: role in reversible protein S-glutathionylation and regulation of redox signal transduction and protein translocation. *Antioxid Redox Signal* 7: 348–366, 2005.
45. Srinivasan U, Mieyal PA, and Mieyal JJ. pH profiles indicative of rate-limiting nucleophilic displacement in thioltransferase catalysis. *Biochemistry* 36: 3199–3206, 1997.
46. Su D and Gladyshev VN. Alternative splicing involving the thioredoxin reductase module in mammals: a glutaredoxin-containing thioredoxin reductase 1. *Biochemistry* 43: 12177–12188, 2004.
47. Su D, Novoselov SV, Sun QA, Moustafa ME, Zhou Y, Oko R, Hatfield DL, and Gladyshev VN. Mammalian selenoprotein thioredoxin-glutathione reductase. Roles in disulfide bond formation and sperm maturation. *J Biol Chem* 280: 26491–26498, 2005.
48. Sutovsky P, Tengowski MW, Navara CS, Zoran SS, and Schatten G. Mitochondrial sheath movement and detachment in mammalian, but not nonmammalian, sperm induced by disulfide bond reduction. *Mol Reprod Dev* 47: 79–86, 1997.
49. Taylor ER, Hurrell F, Shannon RJ, Lin TK, Hirst J, and Murphy MP. Reversible glutathionylation of complex I increases mitochondrial superoxide formation. *J Biol Chem* 278: 19603–19611, 2003.
50. Ursini F, Heim S, Kiess M, Maiorino M, Roveri A, Wissling J, and Flohe L. Dual function of the selenoprotein PHGPx during sperm maturation. *Science* 285: 1393–1396, 1999.
51. Vlamis–Gardikas A and Holmgren A. Thioredoxin and glutaredoxin isoforms. *Methods Enzymol* 347: 286–296, 2002.
52. Xiao R, Lundstrom–Ljung J, Holmgren A, and Gilbert HF. Catalysis of thiol/disulfide exchange. Glutaredoxin 1 and protein-disulfide isomerase use different mechanisms to enhance oxidase and reductase activities. *J Biol Chem* 280: 21099–21106, 2005.
53. Zendman AJW, Ruiter DJ, and van Muijen GNP. Cancer/testis-associated genes: Identification, expression profile, and putative function. *J Cell Physiol* 194: 272–288, 2003.

Address reprint requests to:
Christopher Horst Lillig
Institute for Clinical Cytobiology and Cytopathology
Philipps University
35037 Marburg, Germany

E-mail: horst@lillig.de

Date of first submission to ARS Central, July 5, 2007; date of final revised submission, September 21, 2007; date of acceptance, September 29, 2007.

This article has been cited by:

1. L. Brautigam, L. D. Schutte, J. R. Godoy, T. Prozorovski, M. Gellert, G. Hauptmann, A. Holmgren, C. H. Lillig, C. Berndt. 2011. Vertebrate-specific glutaredoxin is essential for brain development. *Proceedings of the National Academy of Sciences* . [CrossRef]
2. Su-Jung Kim, Hyun-Joo Jung, Hojin Choi, Chang-Jin Lim. 2011. Glutaredoxin 2a, a mitochondrial isoform, plays a protective role in a human cell line under serum deprivation. *Molecular Biology Reports* . [CrossRef]
3. José R. Godoy, Sabrina Oesteritz, Eva-Maria Hanschmann, Wymke Ockenga, Waltraud Ackermann, Christopher Horst Lillig. 2011. Segment-specific overexpression of redoxins after renal ischemia and reperfusion: protective roles of glutaredoxin 2, peroxiredoxin 3, and peroxiredoxin 6. *Free Radical Biology and Medicine* **51**:2, 552-561. [CrossRef]
4. José Rodrigo Godoy, Maria Funke, Waltraud Ackermann, Petra Haunhorst, Sabrina Oesteritz, Francisco Capani, Hans-Peter Elsässer, Christopher Horst Lillig. 2011. Redox atlas of the mouse. *Biochimica et Biophysica Acta (BBA) - General Subjects* **1810**:1, 2-92. [CrossRef]
5. Maria Laura Aon-Bertolino, Juan Ignacio Romero, Pablo Galeano, Mariana Holubiec, Maria Sol Badorrey, Gustavo Ezequiel Saraceno, Eva-Maria Hanschmann, Christopher Horst Lillig, Francisco Capani. 2011. Thioredoxin and glutaredoxin system proteins—immunolocalization in the rat central nervous system. *Biochimica et Biophysica Acta (BBA) - General Subjects* **1810**:1, 93-110. [CrossRef]
6. Young-Mi Go , Dean P. Jones . 2010. Redox Control Systems in the Nucleus: Mechanisms and Functions. *Antioxidants & Redox Signaling* **13**:4, 489-509. [Abstract] [Full Text HTML] [Full Text PDF] [Full Text PDF with Links]
7. Pablo Porras, Brian McDonagh, Jose Rafael Pedrajas, J. Antonio Bárcena, C. Alicia Padilla. 2010. Structure and function of yeast glutaredoxin 2 depend on postranslational processing and are related to subcellular distribution. *Biochimica et Biophysica Acta (BBA) - Proteins and Proteomics* **1804**:4, 839-845. [CrossRef]
8. Margarete Lukosz , Sascha Jakob , Nicole Büchner , Tim-Christian Zschauer , Joachim Altschmied , Judith Haendeler . 2010. Nuclear Redox Signaling. *Antioxidants & Redox Signaling* **12**:6, 713-742. [Abstract] [Full Text HTML] [Full Text PDF] [Full Text PDF with Links]
9. Nicolas Rouhier, Jérémy Couturier, Michael K. Johnson, Jean-Pierre Jacquot. 2010. Glutaredoxins: roles in iron homeostasis. *Trends in Biochemical Sciences* **35**:1, 43-52. [CrossRef]
10. Kevin G. Hoff, Stephanie J. Culler, Peter Q. Nguyen, Ryan M. McGuire, Jonathan J. Silberg, Christina D. Smolke. 2009. In Vivo Fluorescent Detection of Fe-S Clusters Coordinated by Human GRX2. *Chemistry & Biology* **16**:12, 1299-1308. [CrossRef]
11. Christopher Horst Lillig, Roland Lill. 2009. Lights on Iron-Sulfur Clusters. *Chemistry & Biology* **16**:12, 1213-1214. [CrossRef]
12. Yves Meyer, Bob B. Buchanan, Florence Vignols, Jean-Philippe Reichheld. 2009. Thioredoxins and Glutaredoxins: Unifying Elements in Redox Biology. *Annual Review of Genetics* **43**:1, 335-367. [CrossRef]
13. Md. Kaimul Ahsan , Istvan Lekli , Diptarka Ray , Junji Yodoi , Dipak K. Das . 2009. Redox Regulation of Cell Survival by the Thioredoxin Superfamily: An Implication of Redox Gene Therapy in the Heart. *Antioxidants & Redox Signaling* **11**:11, 2741-2758. [Abstract] [Full Text HTML] [Full Text PDF] [Full Text PDF with Links]
14. Aristi P Fernandes, Arrigo Capitanio, Markus Selenius, Ola Brodin, Anna-Klara Rundlöf, Mikael Björnstedt. 2009. Expression profiles of thioredoxin family proteins in human lung cancer tissue: correlation with proliferation and differentiation. *Histopathology* **55**:3, 313-320. [CrossRef]
15. E ARNER. 2009. Focus on mammalian thioredoxin reductases — Important selenoproteins with versatile functions. *Biochimica et Biophysica Acta (BBA) - General Subjects* **1790**:6, 495-526. [CrossRef]
16. Marcia A. Ogasawara , Hui Zhang . 2009. Redox Regulation and Its Emerging Roles in Stem Cells and Stem-Like Cancer Cells. *Antioxidants & Redox Signaling* **11**:5, 1107-1122. [Abstract] [Full Text PDF] [Full Text PDF with Links]
17. Molly M. Gallogly , David W. Starke , John J. Mieyal . 2009. Mechanistic and Kinetic Details of Catalysis of Thiol-Disulfide Exchange by Glutaredoxins and Potential Mechanisms of Regulation. *Antioxidants & Redox Signaling* **11**:5, 1059-1081. [Abstract] [Full Text PDF] [Full Text PDF with Links]
18. Christoph Hudemann , Maria Elisabet Lönn , José Rodrigo Godoy , Farnaz Zahedi Avval , Francisco Capani , Arne Holmgren , Christopher Horst Lillig . 2009. Identification, Expression Pattern, and Characterization of Mouse Glutaredoxin 2 Isoforms. *Antioxidants & Redox Signaling* **11**:1, 1-14. [Abstract] [Full Text PDF] [Full Text PDF with Links]

19. John J. Mieyal , Molly M. Gallogly , Suparna Qanungo , Elizabeth A. Sabens , Melissa D. Shelton . 2008. Molecular Mechanisms and Clinical Implications of Reversible Protein S-Glutathionylation. *Antioxidants & Redox Signaling* **10**:11, 1941-1988. [Abstract] [Full Text HTML] [Full Text PDF] [Full Text PDF with Links]
20. C LILLIG, C BERNDT, A HOLMGREN. 2008. Glutaredoxin systems. *Biochimica et Biophysica Acta (BBA) - General Subjects* **1780**:11, 1304-1317. [CrossRef]